Data Article

Electrochemical data of ferrocenylsubphthalocyanine dyads

Pieter J. Swarts[a], Jeanet Conradie[a],*

[a] Department of Chemistry, PO Box 339, University of the Free State, Bloemfontein, 9300, South Africa

ARTICLE INFO

ABSTRACT

The data presented in this paper is related to the research article entitled "*Synthesis, Spectroscopy, Electrochemistry and DFT of Electron-Rich Ferrocenylsubphthalocyanines*" [1] where electrochemical redox data and cyclic voltammograms at only a scan rate of 0.10 V s^{-1} of four ferrocenylsubphthalocyanine dyads $Fc(CH_2)_nCO_2BSubPc(H)_{12}$ ($n = 0$, 1 or 3) and $FcCO(CH_2)_2CO_2BSubPc(H)_{12}$, are presented. This data article provides extensive electrochemical redox data and cyclic voltammograms at various scan rates from 0.05 up to 5.00 V s^{-1} to illustrate the effect of the different scan rates on the electrochemical behaviour of the four ferrocenylsubphthalocyanine dyads.

---

* Corresponding author.
 E-mail address: conradj@ufs.ac.za (J. Conradie).

Specifications Table

Subject	Chemistry
Specific subject area	Electrochemistry
Type of data	Cyclic voltammogram
	Table
How data were acquired	On an electrochemical analyser connected to a desktop computer, as described in the experimental details.
Data format	Raw
	Analysed
Parameters for data collection	Pure samples as synthesized.
Description of data collection	All electrochemical experiments were done in 2 ml cell containing three electrodes as described in the experimental details, was used to obtain the CVs.
Data source location	Institution: University of the Free State
	City/Town/Region: Bloemfontein
	Country: Republic of South Africa
Data accessibility	In the article and supporting data.
Related research article	P.J. Swarts, J. Conradie, Synthesis, Spectroscopy, Electrochemistry and DFT of Electron-Rich Ferrocenylsubphthalocyanines, Molecules. 25 (2020) 2575. doi:10.3390/molecules25112575 [1]

Value of the Data

- The electrochemical data of four ferrocenylsubphthalocyanine dyads may used by chemical researchers in the development of macrocyclic compounds such as subphthalocyanines, porphyrins and phthalocyanines.
- This data article illustrates the effect of different scan rates (up to 5.0 Vs^{-1}) on the experimental cyclic voltammograms and the related electrochemical data of four ferrocenylsubphthalocyanine dyads.
- This data illustrates the effect of different axial ligands $L = Fc(CH_2)_nCO_2$ ($n = 0$, 1 or 3) or $FcCO(CH_2)_2CO_2$, on the formal reduction potential of the ferrocenyl oxidation, the first macrocycle based oxidation and the first macrocycle based reduction of subphthalocyanines L-$BSubPc(H)_{12}$.
- This data illustrates the effect of the aromatic macrocycle of the subphthalocyanine L-$BSubPc(H)_{12}$ and of the alkyl chain length between B and Fc on the $Fe^{II/III}$ oxidation potential of the ferrocenyl group of the ferrocenylcarboxylic acid moieties, $L = Fc(CH_2)_nCO_2$ ($n = 0$, 1 or 3) or $FcCO(CH_2)_2CO_2$, for four ferrocenylsubphthalocyanine dyads.
- The ferrocenyl group on the axial ligand of a subphthalocyanine, influences the optical and electrochemical properties of the ferrocenylsubphthalocyanine dyads. Data of this article illustrate how different axial ligands change the redox properties of ferrocenylsubphthalocyanine dyads as may be needed for different applications such as for solar energy applications, sensors and photodynamic therapy. Knowledge of detailed redox data of both the $Fe^{II/III}$ and macrocycle based oxidation and reduction processes, of as many as possible different ferrocenylsubphthalocyanine dyads can assist in future research in designing ferrocenylsubphthalocyanine dyads with specific electrochemical properties.

1. Data Description

We previously reported the electrochemical data of two fluorinated ferrocenylsubphthalocyanines $(Fc(CH_m)_nCOO)$-$BSubPc(F)_{12}$ (m = 1 or 2 and n = 2) and their non-fluorinated analogues [2]. Here we report detailed electrochemical data of four different ferrocenyl-subphthalocyanines $Fc(CH_m)_nCO_2BSubPc(H)_{12}$ (m = 2 and n = 0, 1 or 3) and

Table 1

Electrochemical data (potential in V vs Fc/Fc+) in DCM for 5×10^{-4} mol dm−3 of FcCO2BSubPc(H)12 at indicated scan rates (ν in V/s). See Fig. 3 for peak assignments.

ν (V/s)	$E_p{}^a$ / V	ΔE_p / V	$E^{o'}$ / V	$i_p{}^b$ / μA	i_p ratio^c	$E_p{}^a$ / V	ΔE_p / V	$E^{o'}$ / V	$i_p{}^b$ / μA	i_p ratio^c
		1st oxidation (Fc)						2nd oxidation (I)		
0.050	0.262	0.075	0.224	2.58	0.99	0.710	0.081	0.670	2.39	0.99
0.200	0.262	0.077	0.224	5.05	0.99	0.711	0.083	0.670	4.68	0.99
0.300	0.263	0.078	0.224	5.78	0.99	0.712	0.084	0.670	5.34	0.99
0.400	0.263	0.079	0.224	8.30	0.99	0.712	0.085	0.670	7.68	0.99
0.500	0.264	0.080	0.224	9.03	0.99	0.713	0.086	0.670	8.35	0.99
5.000	0.265	0.082	0.224	16.34	0.99	0.714	0.088	0.670	23.97	0.99
		1st reduction (II)						2nd reduction (III)		
0.050	-1.642	0.083	-1.601	2.48	0.99	-2.123	-	-	-	-
0.200	-1.643	0.085	-1.601	4.86	0.99	-2.124	-	-	-	-
0.300	-1.644	0.086	-1.601	5.55	0.99	-2.125	-	-	-	-
0.400	-1.644	0.087	-1.601	7.98	0.99	-2.125	-	-	-	-
0.500	-1.645	0.088	-1.601	8.68	0.99	-2.126	-	-	-	-
5.000	-1.646	0.090	-1.601	22.75	0.99	-2.127	-	-	-	-

[a] E_p = peak anodic potential for oxidation (E_{ox}) and peak cathodic potential for reduction (E_{red}).
[b] i_p is the peak anodic current for oxidation (i_{pa}) and peak cathodic current for reduction (i_{pc}).
[c] i_p ratio = i_{pc}/i_{pa} (oxidation peak) or i_{pa}/i_{pc} (reduction peak).

Table 2

Data for 5×10^{-4} mol dm^{-3} of FcCH$_2$CO$_2$BSubPc(H)$_{12}$. See caption and footnote at Table 1 for details. See Fig. 4 for peak assignments.

ν (V/s)	$E_p{}^a$ / V	ΔE_p / V	$E^{o'}$ / V	$i_p{}^b$ / μA	i_p ratio^c	$E_p{}^a$ / V	ΔE_p / V	$E^{o'}$ / V	$i_p{}^b$ / μA	i_p ratio^c
		1st oxidation (Fc)						2nd oxidation (I)		
0.050	-0.005	0.075	-0.043	2.58	0.99	0.709	0.079	0.670	2.41	0.99
0.200	-0.004	0.077	-0.043	5.05	0.99	0.710	0.081	0.670	4.73	0.99
0.300	-0.004	0.078	-0.043	5.78	0.99	0.711	0.082	0.670	5.41	0.99
0.400	-0.003	0.079	-0.043	8.30	0.99	0.711	0.083	0.670	7.77	0.99
0.500	-0.003	0.080	-0.043	9.03	0.99	0.712	0.084	0.670	8.45	0.99
5.000	-0.002	0.082	-0.043	16.14	0.99	0.713	0.088	0.670	23.21	0.99
		1st reduction (II)						2nd reduction (III)		
0.050	-1.642	0.081	-1.674	2.49	0.99	-2.153	-	-	-	-
0.200	-1.643	0.083	-1.674	4.89	0.99	-2.154	-	-	-	-
0.300	-1.644	0.084	-1.674	5.58	0.99	-2.155	-	-	-	-
0.400	-1.644	0.085	-1.674	8.03	0.99	-2.155	-	-	-	-
0.500	-1.645	0.086	-1.674	8.73	0.99	-2.156	-	-	-	-
5.000	-1.646	0.088	-1.674	23.36	0.99	-2.157	-	-	-	-

FcCO(CH$_2$)$_2$CO$_2$BSubPc(H)$_{12}$, see Fig. 1. The ferrocenyl-subphthalocyanines of this study contain ferrocenylcarboxylic acids with different alkyl chain lengths as axial ligands to illustrate the influence of the chain length and type on the observed redox behaviour of the complexes. The electrochemical data of the four ferrocenylsubphthalocyanine dyads, FcCO$_2$BSubPc(H)$_{12}$, FcCH$_2$CO$_2$BSubPc(H)$_{12}$, Fc(CH$_2$)$_3$CO$_2$BSubPc(H)$_{12}$ and FcCO(CH$_2$)$_2$CO$_2$BSubPc(H)$_{12}$, shown in Fig. 1, are reported in Tables 1–4 and the cyclic voltammograms (CVs) at various scan rates shown Figs. 2–6. The raw current – potential data is available in the supplementary files uploaded. The electrochemical data and CVs at a scan rate of 0.100 V s^{-1}, are provided in the related research article [1]. All CVs show one Fe based and one macrocycle based oxidation and two macrocycle based reductions for the four SubPcs, similar as was observed for the ferrocenylsubphthalocyanine dyads FcCH$_2$OBSubPc(H)$_{12}$ [3], FcCO$_2$BSubPc(H)$_{12}$ [3], FcBSubPc(H)$_{12}$ [4], FcC≡CBSubPc(H)$_{12}$ [4], Fc(CH$_2$)$_2$CO$_2$BSubPc(X)$_{12}$ and Fc(CH)$_2$CO$_2$BSubPc(X)$_{12}$ with X = H or F [2,5]. The decreasing trend of redox potential of the iron based oxidation, with increasing alkyl
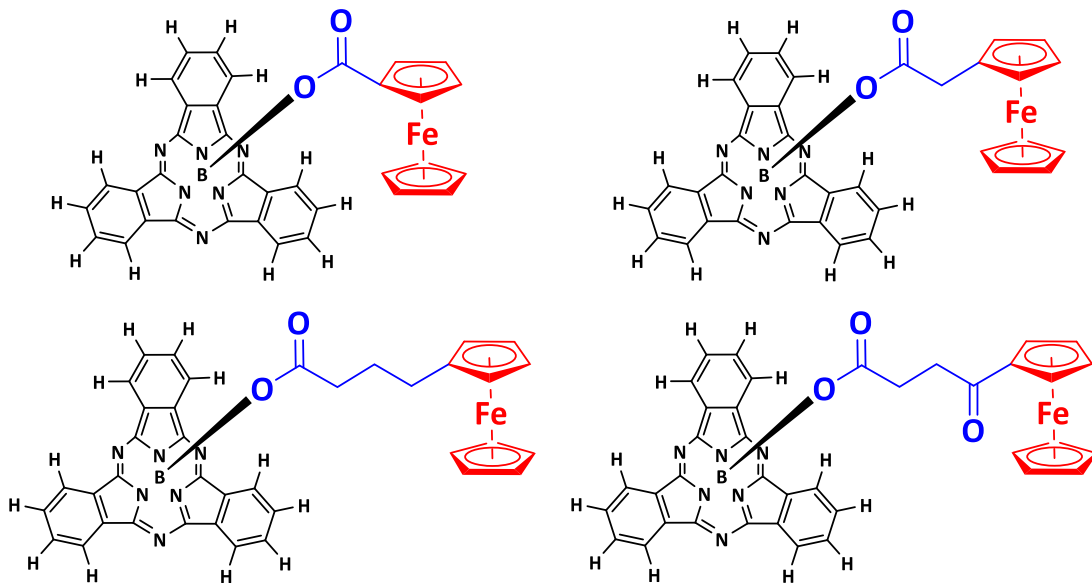
Fig. 1. Ferrocenylsubphthalocyanine dyads of which the electrochemical data is reported in this study.

Table 3

Data for 5×10^{-4} mol dm^{-3} of Fc(CH$_2$)$_3$CO$_2$BSubPc(H)$_{12}$. See caption and footnote at Table 1 for details. See Fig. 5 for peak assignments.

ν (V/s)	$E_p{}^a$ / V	ΔE_p / V	$E^{o'}$ / V	$i_p{}^b$ / μA	i_p ratio^c	$E_p{}^a$ / V	ΔE_p / V	$E^{o'}$ / V	$i_p{}^b$ / μA	i_p ratio^c
		1st oxidation (Fc)						2nd oxidation (I)		
0.050	-0.024	0.075	-0.062	2.56	0.99	0.710	0.081	0.670	2.34	0.99
0.200	-0.023	0.077	-0.062	5.01	0.99	0.711	0.083	0.670	4.58	0.99
0.300	-0.023	0.078	-0.062	5.73	0.99	0.712	0.084	0.670	5.23	0.99
0.400	-0.022	0.079	-0.062	8.23	0.99	0.712	0.085	0.670	7.52	0.99
0.500	-0.022	0.080	-0.062	8.95	0.99	0.713	0.086	0.670	8.18	0.99
5.000	-0.021	0.082	-0.062	16.57	0.99	0.714	0.088	0.670	23.48	0.99
		1st reduction (II)						2nd reduction (III)		
0.050	-1.870	0.083	-1.829	2.42	0.99	-2.343	-	-	-	-
0.200	-1.871	0.085	-1.829	4.75	0.99	-2.344	-	-	-	-
0.300	-1.872	0.086	-1.829	5.42	0.99	-2.345	-	-	-	-
0.400	-1.872	0.087	-1.829	7.80	0.99	-2.345	-	-	-	-
0.500	-1.873	0.088	-1.829	8.48	0.99	-2.346	-	-	-	-
5.000	-1.874	0.090	-1.829	22.92	0.99	-2.347	-	-	-	-

Table 4

Data for 5×10^{-4} mol dm^{-3} of FcCO(CH$_2$)$_2$CO$_2$BSubPc(H)$_{12}$. See caption and footnote at Table 1 for details. See Fig. 6 for peak assignments.

ν (V/s)	$E_p{}^a$ / V	ΔE_p / V	$E^{o'}$ / V	$i_p{}^b$ / μA	i_p ratio^c	$E_p{}^a$ / V	ΔE_p / V	$E^{o'}$ / V	$i_p{}^b$ / μA	i_p ratio^c
		1st oxidation (Fc)						2nd oxidation (I)		
0.050	0.300	0.075	0.262	2.55	0.99	0.710	0.081	0.670	2.39	0.99
0.200	0.300	0.077	0.262	5.00	0.99	0.711	0.083	0.670	4.69	0.99
0.300	0.301	0.078	0.262	5.71	0.99	0.712	0.084	0.670	5.36	0.99
0.400	0.301	0.079	0.262	8.21	0.99	0.712	0.085	0.670	7.71	0.99
0.500	0.302	0.080	0.262	8.93	0.99	0.713	0.086	0.670	8.38	0.99
5.000	0.303	0.082	0.262	16.73	0.99	0.714	0.087	0.670	23.72	0.99
		1st reduction (II)						2nd reduction (III)		
0.050	-1.524	0.085	-1.482	2.44	0.99	-2.003	-	-	-	-
0.200	-1.525	0.087	-1.482	4.77	0.99	-2.004	-	-	-	-
0.300	-1.526	0.088	-1.482	5.46	0.99	-2.005	-	-	-	-
0.400	-1.526	0.089	-1.482	7.84	0.99	-2.005	-	-	-	-
0.500	-1.527	0.090	-1.482	8.53	0.99	-2.006	-	-	-	-
5.000	-1.528	0.092	-1.482	23.15	0.99	-2.007	-	-	-	-

chain length n in Fc(CH$_2$)$_n$CO$_2$BSubPc(H)$_{12}$ (n = 0–3) is similar to the trend of the oxidation of iron in the free ferrocenylcarboxylic acids Fc(CH$_2$)$_n$CO$_2$H [6]. Reported first macrocycle based oxidation of the SubPcs generally exhibits irreversible behaviour [4,7], however, introduction of a ferrocenylcarboxylic acid moiety in the axial position of the subphthalocyanine L-BSubPc(H)$_{12}$, led to chemically reversible behaviour (peak current ratios of 1) and with peak current voltage separations of $\Delta E < 0.092$ V [1,2,5].

2. Experimental Design, Materials and Methods

The experimental setup is as described earlier [5], namely: All electrochemical measurements (cyclic voltammetry) were obtained at RT (25°C) on 5×10^{-4} mol dm^{-3} analyte solution in anhydrous dichloromethane with 0.1 mol dm^{-3} tetrabutylammonium tetrakispentafluorophenylborate, [N(^{n}Bu)$_4$][B(C$_6$F$_5$)$_4$] as supporting electrolyte under an Ar atmosphere (H$_2$O and O$_2$ < 10 ppm) in a glove box (MBraun Lab Master SP), utilizing a Princeton Applied Research PARSTAT 2273 potentiostat with the Powersuite software (Version 2.58). A cell containing
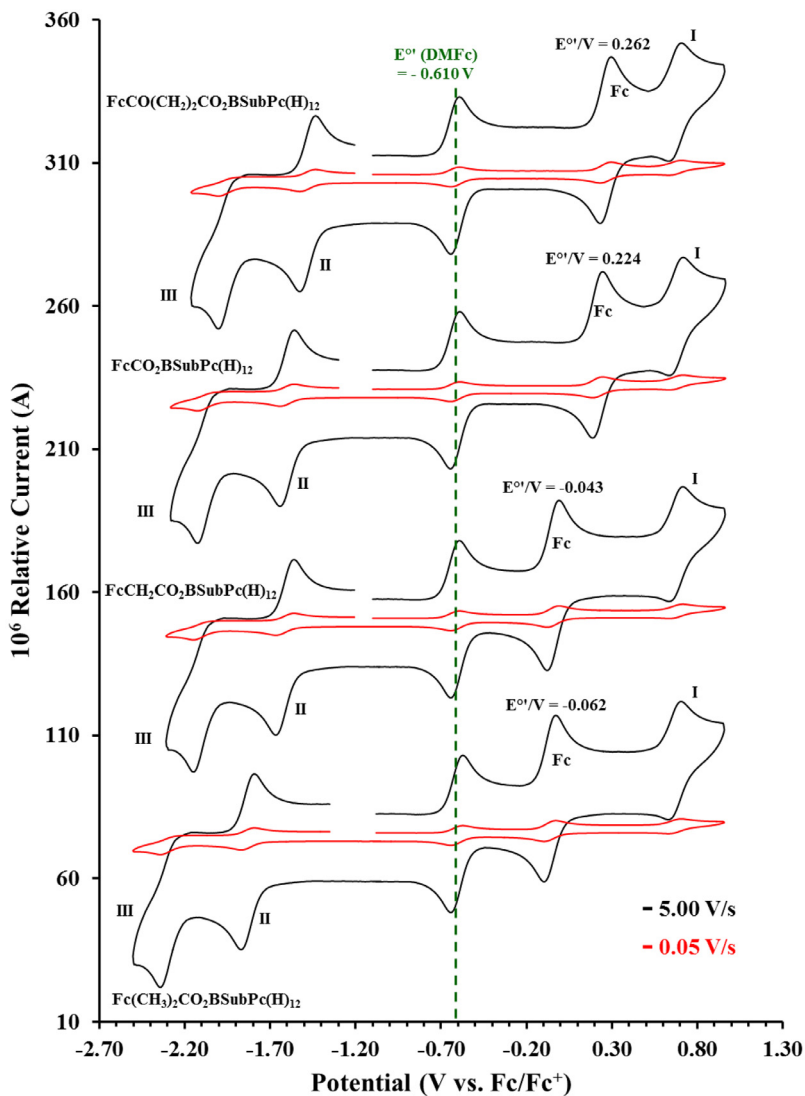
Fig. 2. From top to bottom: Cyclic voltammograms (CVs) of 5×10^{-4} mol dm−3 of FcCO(CH2)2CO2-BSubPc(H)12, FcCO2-BSubPc(H)12, FcCH2CO2-BSubPc(H)12 and Fc(CH2)3CO2-BSubPc(H)12 at the indicated scan rates (Vs−1), in dichloromethane as solvent. Supporting electrolyte = 0.1 mol dm−3 [N(nBu)4][B(C6F5)4]. Scans initiated from ca -1 V in a positive direction. E0' of the internal standard DMFc is indicated with a green dashed line. E0' of the ferrocenyl oxidation of the indicated ferrocenylsubphthalocyanine dyads (labelled as Fc) is given in V.

three electrodes was used to obtain the CVs, namely a working electrode (glassy C), an auxiliary electrode (Pt wire) and a reference electrode (Pt wire). Decamethylferrocene ($E^{\circ\prime} = -0.610$ V vs. Fc/Fc+) was used as internal reference, with the data reported vs. the ferrocene/ferrocenium redox couple as suggested by IUPAC [8]. Before each scan the glassy C electrode was prepared as follow: (i) polish on a Buhler polishing mat with 1-micron and with ¼-micron diamond paste, (ii) rinsed with distilled water, acetone and dichloromethane, and (iii) dried.
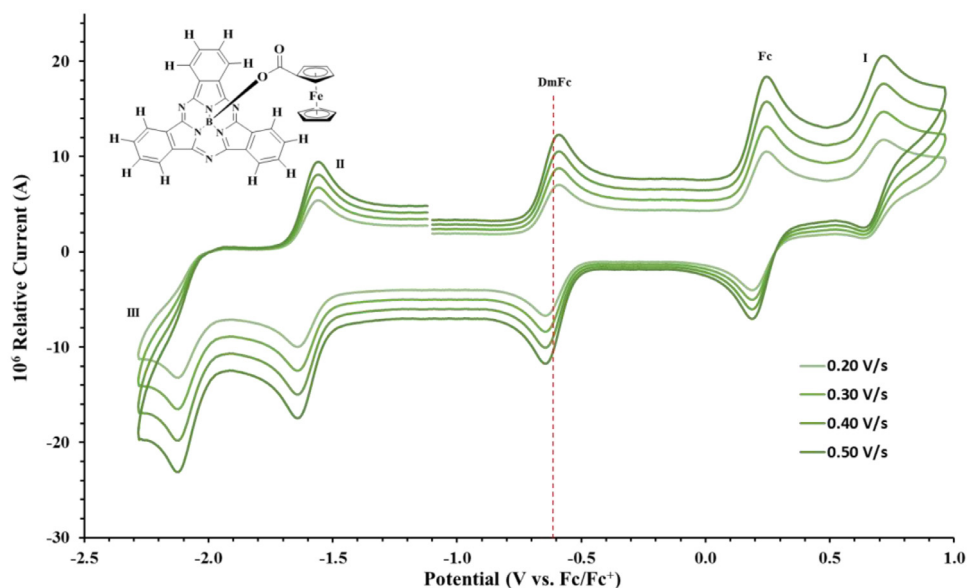
Fig. 3. CVs of 5 × 10^{-4} mol dm−3 of FcCO2BSubPc(H)12 at scan rates of 0.20, 0.30, 0.40 and 0.50 Vs−1, in dichloromethane as solvent and 0.1 mol dm−3 [N(nBu)4][B(C6F5)4] as supporting electrolyte. Scans initiated from ca -1.1 V in a positive direction. E0' of the internal standard DMFc is indicated with a red dashed line.
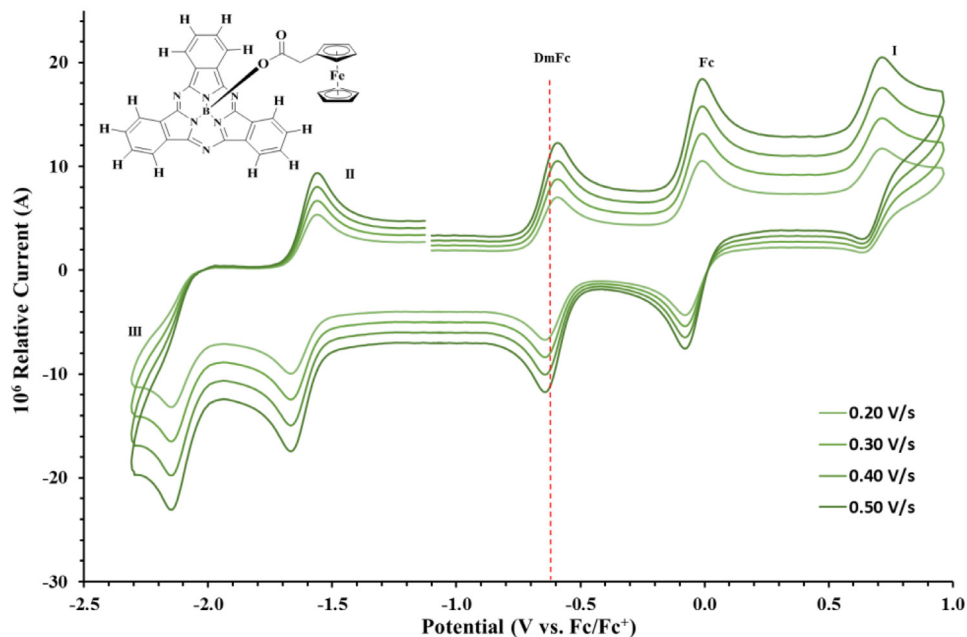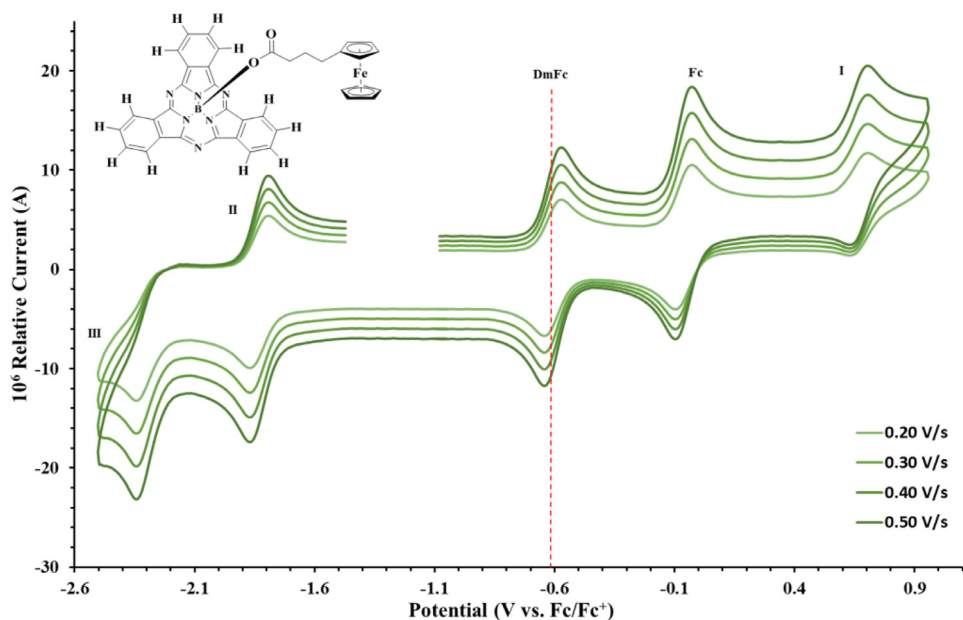

Fig. 4. CVs of 5 × 10^{-4} mol dm−3 of FcCH2CO2BSubPc(H)12 at scan rates of 0.20, 0.30, 0.40 and 0.50 Vs−1, in dichloromethane as solvent and 0.1 mol dm−3 [N(nBu)4][B(C6F5)4] as supporting electrolyte. Scans initiated from ca -1.1 V in a positive direction. E0' of the internal standard DMFc is indicated with a red dashed line.
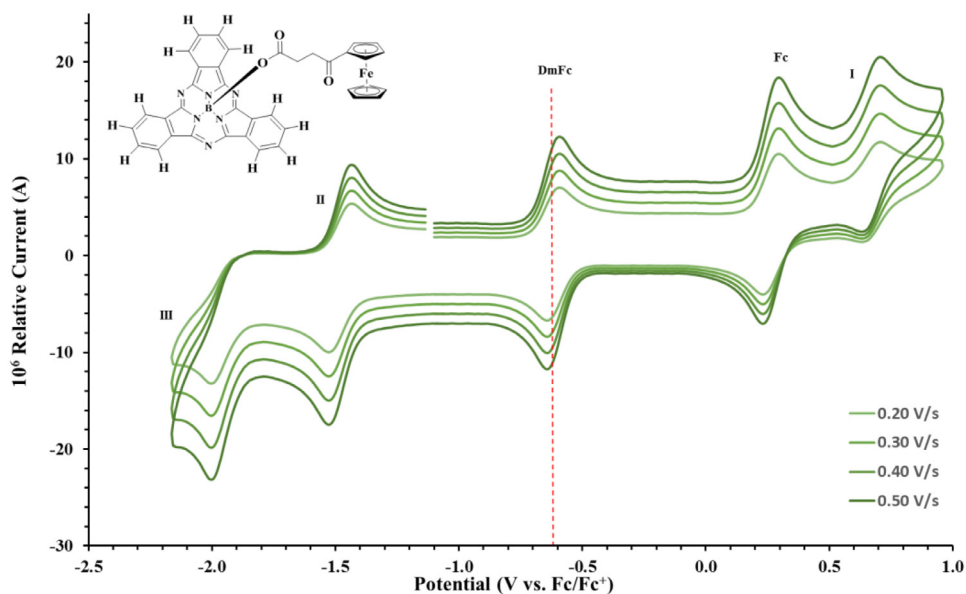
Fig. 5. CVs of 5 × 10^{-4} mol dm−3 of Fc(CH2)3CO2BSubPc(H)12 at scan rates of 0.20, 0.30, 0.40 and 0.50 Vs−1, in dichloromethane as solvent and 0.1 mol dm−3 [N(nBu)4][B(C6F5)4] as supporting electrolyte. Scans initiated from ca -1.1 V in a positive direction. E0' of the internal standard DMFc is indicated with a red dashed line.

Fig. 6. CVs of 5 × 10^{-4} mol dm−3 of FcCO(CH2)2CO2BSubPc(H)12 at scan rates of 0.20, 0.30, 0.40 and 0.50 Vs−1, in dichloromethane as solvent and 0.1 mol dm−3 [N(nBu)4][B(C6F5)4] as supporting electrolyte. Scans initiated from ca -1.1 V in a positive direction. E0' of the internal standard DMFc is indicated with a red dashed line.

Ethics Statement

This work does not require any ethical statement.

Declaration of Competing Interest

The authors declare that they have no known competing financial interests or personal relationships which have, or could be perceived to have, influenced the work reported in this article.

Acknowledgments

Supplementary materials

Supplementary material associated with this article can be found, in the online version, at doi:10.1016/j.dib.2020.106245.

Supplementary files

Voltage-current data of all CVs in Excel files.

References

[1] P.J. Swarts, J. Conradie, Synthesis, spectroscopy, electrochemistry and DFT of Electron-Rich Ferrocenylsubphthalocyanines, Molecules 25 (2020) 2575, doi:10.3390/molecules25112575.

[2] P.J. Swarts, J. Conradie, Oxidation and reduction data of four subphthalocyanines with axially coordinated ferrocenylcarboxylic acids, Data Br. 31 (2020) 105816, doi:10.1016/j.dib.2020.105816.

[3] P.V. Solntsev, K.L. Spurgin, J.R. Sabin, A.A. Heikal, V.N. Nemykin, Photoinduced Charge Transfer in Short-Distance Ferrocenylsubphthalocyanine Dyads, Inorg. Chem. 51 (2012) 6537–6547, doi:10.1021/ic3000608.

[4] E. Maligaspe, M.R. Hauwiller, Y.V. Zatsikha, J.A. Hinke, P.V. Solntsev, D.A. Blank, V.N. Nemykin, Redox and photoinduced electron-transfer properties in short distance organoboryl ferrocene-subphthalocyanine dyads, Inorg. Chem. 53 (2014) 9336–9347, doi:10.1021/ic5014544.

[5] P.J. Swarts, J. Conradie, Redox and photophysical properties of four subphthalocyanines containing ferrocenylcarboxylic acid as axial ligands, Inorg. Chem. 59 (2020) 7444–7452, doi:10.1021/acs.inorgchem.0c00150.

[6] P.J. Swarts, J. Conradie, Solvent and substituent effect on electrochemistry of ferrocenylcarboxylic acids, J. Electroanal. Chem. 866 (2020) 114164, doi:10.1016/j.jelechem.2020.114164.

[7] C.G. Claessens, D. González-Rodríguez, M.S. Rodríguez-Morgade, A. Medina, T. Torres, Subphthalocyanines, Subporphyrazines, and Subporphyrins: Singular Nonplanar Aromatic Systems, Chem. Rev. 114 (2014) 2192–2277, doi:10.1021/cr400088w.

[8] G. Gritzner, J. Kuta, Recommendations on reporting electrode potentials in nonaqueous solvents (Recommendations 1983), Pure Appl. Chem. 56 (1984) 461–466, doi:10.1351/pac198456040461.